

Effect of long- and short-term exposure to laser light at 1070 nm on growth of *Saccharomyces cerevisiae*

Thomas Aabo

University of Copenhagen
Department of Food Science
Rolighedsvej 30
Frederiksberg 1958
Denmark

Ivan R. Perch-Nielsen

DTU Nanotech
Technical University of Denmark
Department of Micro- and Nanotechnology
Kongens Lyngby, 2800
Denmark

Jeppe Seidelin Dam

Darwin Z. Palima

DTU Fotonik
Technical University of Denmark
Department of Photonics Engineering
Kongens Lyngby, 2800
Denmark

Henrik Siegumfeldt

University of Copenhagen
Department of Food Science
Rolighedsvej 30
Frederiksberg 1958
Denmark

Jesper Glückstad

DTU Nanotech
Technical University of Denmark
Department of Micro- and Nanotechnology
Kongens Lyngby, 2800
Denmark

Nils Arneborg

University of Copenhagen
Department of Food Science
Rolighedsvej 30
Frederiksberg 1958
Denmark

1 Introduction

Until just a few years ago, virtually all laser manipulation schemes were based on the principle of trapping particles inside a single strongly focused beam and then subsequently moving to a desired position by translating the microscope stage. With the advent of computer-addressable spatial light modulators (SLMs) and acousto-optic deflectors (AODs), much more versatile manipulation of multiple particles and

Abstract. The effect of a 1070-nm continuous and pulsed wave ytterbium fiber laser on the growth of *Saccharomyces cerevisiae* single cells is investigated over a time span of 4 to 5 h. The cells are subjected to optical traps consisting of two counterpropagating plane wave beams with a uniform flux along the x , y axis. Even at the lowest continuous power investigated—i.e., 0.7 mW—the growth of *S. cerevisiae* cell clusters is markedly inhibited. The minimum power required to successfully trap single *S. cerevisiae* cells in three dimensions is estimated to be 3.5 mW. No threshold power for the photodamage, but instead a continuous response to the increased accumulated dose is found in the regime investigated from 0.7 to 2.6 mW. Furthermore, by keeping the delivered dose constant and varying the exposure time and power—i.e. pulsing—we find that the growth of *S. cerevisiae* cells is increasingly inhibited with increasing power. These results indicate that growth of *S. cerevisiae* is dependent on both the power as well as the accumulated dose at 1070 nm. © 2010 Society of Photo-Optical Instrumentation Engineers. [DOI: 10.1117/1.3430731]

Keywords: laser-induced damage; infrared lasers; cells.

Paper 09303PRR received Jul. 22, 2009; revised manuscript received Jan. 7, 2010; accepted for publication Jan. 11, 2010; published online Jul. 6, 2010.

cells is now possible by using tailored structures of light^{1,2} to organize microorganisms in desired patterns.³ These techniques open up for promising themes of interdisciplinary studies including those of biological and medical relevance, which are now viable using reconfigurable patterns of optical fields.⁴ The use of confining optical potential landscapes is made even more feasible by implementing a great degree of interactive user control into real-time reconfigurable trapping and manipulation.⁵

The first successful optical tweezing was shown in 1987

Address all correspondence to: Thomas Aabo, Department of Food Science, University of Copenhagen, Rolighedsvej 30, 1958, Frederiksberg C, Denmark. Tel: 45-35-333636. Fax: 45-35-333214; E-mail: taa@life.ku.dk

using an infrared (IR) laser (1064-nm ND:YAG) of both *Escherichia coli* and *Saccharomyces cerevisiae*.⁶ The move from visible lasers to near-IR lasers was favorable as the near-IR waveband is comparatively transparent to biological material along with a relatively low absorption in water; therefore, reducing cell damage caused by optical trapping considerably.⁷ However, the use of highly focused IR laser beams is not without consequences to the state of the trapped cells, as photodamage will still occur.

The wavelength dependency of the induced photodamage in cells has been characterized by examining the cloning efficiency of Chinese hamster ovary (CHO) cells,⁸ the rotation rate of the *E. coli* flagella motor,⁹ and the green fluorescent protein (GFP) gene expression in *E. coli*.¹⁰ The two first studies found two wavebands around 830 and 970 nm, which were significantly less harmful to cells, and a specifically harmful region from 870 to 910 nm. The 1064-nm wavelength was found to be as harmful for CHO cells as 900 nm, while the *E. coli* cells were less affected at 1064 nm than at the harmful regions from 870 to 910 nm. Mirsaidov et al.,¹⁰ however, found that GFP expression in *E. coli* exposed to laser light from 840 to 930 nm was only weakly affected. The discrepancies between the results of these studies could be due to the different physiological parameters measured and/or the organisms used.

Recently, using 1064 nm, it was shown that *E. coli* cell damage was linearly dependent on the total dose received and that the growth rate was adversely affected at a dose of 0.5 J, while cell division ability was affected¹¹ at an even lower dose of 0.35 J. However, Mohanty et al. found DNA damage in human lymphoblasts to be dependent not only on total dose but also on peak power.¹² By using the intracellular pH (pH_i) as a measure of viability, it was recently discovered¹³ that the pH_i of both *E. coli* and *Listeria* declined at trapping powers as low as 6 mW. Furthermore, it was shown that a dose of 5 J caused 50% lethality in exposed *E. coli* cells.¹⁰

Very recently, it was shown that time lapse fluorescence imaging at 470 nm caused light-induced stress in *S. cerevisiae*.¹⁴ To our knowledge, there are no quantitative studies on the effect of laser light at a wavelength near 1064 nm on yeast cell growth. Here, we investigate the effects of trapping with a 1070-nm continuous and pulsed wave Ytterbium fiber laser on growth of *S. cerevisiae* single cells over a time span of 4 to 5 h.

2 Materials and Methods

2.1 Yeast Strains and Growth Conditions

Saccharomyces cerevisiae (Saint Georges S101, Bio Springer, France) was used for all experiments. Cells were grown in YPG medium (glucose 10 g/L, pH 5.6) at 25 °C under shaking (120 rpm), harvested in the midexponential phase (concentration: 5×10^5 cells/ml), and transferred to a growth chamber (see in the following), where they were left to settle and attach to the surface for 5 min. Subsequently, the growth chamber was flushed with fresh YPG medium to remove any cells not attached to the surface, which could diffuse into the field of view and interfere with measurements.

The growth chamber used for the experiments consisted of a cover glass slide (Menzel-Gläser #1; 0.15 mm; size, 24

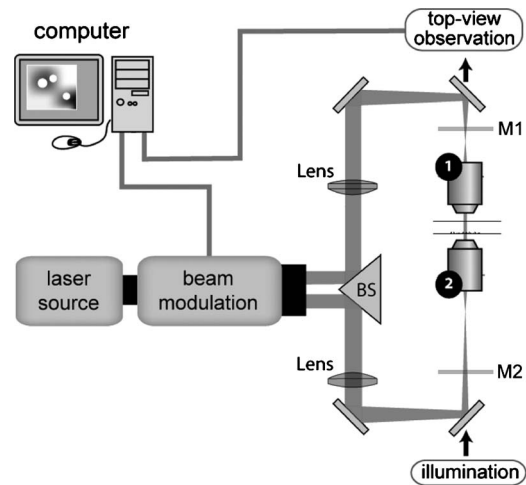


Fig. 1 Biophotonics workstation. The beam from the laser source is sent to the beam modulation and is split into two beam arrays that are, respectively, diverted to the upper and lower objective by the beam-splitter (BS) and four mirrors. In this study, the separation between objectives 1 and 2 is 1.2 cm. M1 and M2 are measurement points for laser power.

$\times 40$ mm) and a perfusion chamber (CoverWell, Grace-BioLab). The cover glass slides were first cleaned in 70% ethanol, 1% HCl, and then washed with demineralized water and left to dry. The cover glass slides were coated with a 0.8 mg/ml solution of concanavalin A (0.5 ml per cover glass) and left to dry. Once dry, the CoverWell perfusion chamber was attached to the coated cover glass slides, and sealed with adhesive tape. The presence of Concanavalin A did not affect the growth rate of the cells (data not shown).

2.2 BioPhotonics Workstation

The biophotonics workstation¹⁵ (BWS) used in this work is illustrated schematically in Fig. 1. It employs an optical mapping from a beam modulation module to obtain reconfigurable patterns corresponding to two independently addressable regions which are relayed to a BS, creating the two opposing beam patterns that are sent into the sample. The addressable regions occupied approximately half the field of view of the camera. The spatial addressing of the expanded laser source is done in real time through a high-speed computer-controlled SLM that is integrated in the beam modulation module (patent pending). Through a computer interface, the operator can simply select, trap, and move the desired objects with a mouse. The trap sizes can also easily be changed in diameter. The pattern created in the trapping region in the chamber was homogenous across the x - y plane, and the trapping power is not dependent on the number of traps created. The generated array of counterpropagating trapping beams is then easily aligned using a computer-guided alignment procedure.¹⁶

The laser used in the experiments is a ytterbium fiber laser with a central wavelength of 1070 nm (IPG photonics, type: YLM-20-SC). It has a maximal output power of $P_{\text{output(max)}} = 20$ W. The camera used for top-view observation is a JAI CV-A10GE (800 \times 600 pixels). Two identical objectives were used. These were long-working-distance air objectives optimized for IR (Olympus, LMPlan 50 \times IR, nu-

merical aperture 0.55), which generated a large field of view and the long working distance of 6 mm leaves space for integrating other enabling tools for probing the trapped particles, such as linear and nonlinear microscopy or microspectroscopy.¹⁷ However, one is not restricted to using long-working-distance (LWD) objectives and they can easily be replaced with high-numerical-aperture (NA) objectives offering a higher resolution, at the cost of a smaller field of view.

To measure the transmittance we used a dual-objective transmittance technique¹⁸ whereby the laser is sent through oppositely aligned facing objectives. This technique was used because it required the least amount of adjustment of the setup. The power (P_1) of the beam was measured at M1 and P_2 was measured at M2 after passing through the objectives (see Fig. 1). The transmittance coefficient of a single objective (τ_{obj}) is then the square root of P_2/P_1 . The transmittance through a single objective (τ_{obj}) was measured to be $\tau_{obj} = 0.75$. The transmittance coefficient at 1064 nm of the cover glass (τ_{cov}) was specified by the manufacturer at $\tau_{cov} = 0.92$. We assume that the shift in wavelength to 1070 nm does not change the value of τ_{cov} significantly.

2.3 Flux Calculation

Because of the technique used in the BWS, the laser power is evenly distributed across the trapping area. This is different from single-beam optical tweezers, which focus the laser to a diffraction limited spot. To calculate the flux at the specimen plane we measured the power (Φ_{obj}) just before the objectives at M1, as seen in Fig. 1, at multiple trap sizes. This gave us the conversion factor (Y_{conv}) (μm^{-2}) accounting for both attenuation and scaling of the laser beam through the setup. The flux in the specimen plane ($E_{specimen}$) is then given by

$$E_{specimen} = \tau_{cov} \tau_{obj} Y_{conv} P_{output},$$

where P_{output} is the laser output power. Multiplying the flux with the cell area (A_{cell}) gives the power through the cell (Φ_{cell}).

$$\Phi_{cell} = E_{specimen} A_{cell}.$$

Using the image-processing technique stated in Sec. 2.6, we measured the average cell area of a fully grown single yeast cell to be $A_{cell} = 21 \mu\text{m}^2$, with a standard deviation of $\pm 2 \mu\text{m}^2$. With a flux of $0.024 \text{ mW}/\mu\text{m}^2$ per laser output watt (P_{output}), the maximum power through a yeast cell was $\Phi_{cell,max} = 10 \text{ mW}$. We chose to display the data as a function of the power through a cell, rather than the flux. This was done to enable a direct comparison of the power through cells, between optical tweezers with highly focused traps, and the BWS. In the pulse experiments, the yeast cells were irradiated for a specific time (t_{exp}). The dose D (in joules) received by an average cell was then given by $D = \Phi_{cell} t_{exp}$.

2.4 Determination of Cell Area Index

Once the growth chamber was flushed and sealed, it was put under the microscope. After visual inspection, a number of cells was found within close proximity to each other and as close to the same stage in the cell cycle as possible. The stage in the cell cycle was determined by the size of an emerging

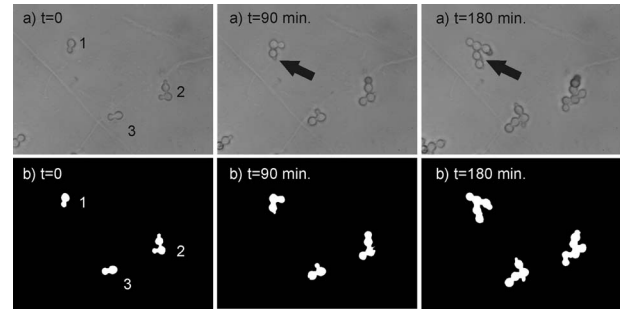


Fig. 2 (a) Original and (b) thresholded images of a single growth experiment. In the thresholded images, the area occupied by the ROI is represented by a white color. The cells within ROI 1 are the control cells. The cells within ROIs 2 and 3 were irradiated for 10 min at a power of 5 mW. The black arrows show the appearance of two consecutive buds from the same mother cell.

bud. Images were taken at the start of irradiation at $t=0$, and consequently every 2 min. Image analysis was performed on images selected at 30-min intervals.

To measure the cell growth as a function of time, the area occupied by all cells within a region of interest (ROI) was extracted from every image. The ROI was defined as the cells that were all originating from the same mother cell. The area occupied by all cells within an ROI was given by the number of pixels (NoP) that it occupied in a picture after image processing and thresholding, as seen in Fig. 2(b). Figure 2 shows the growth of cells within three ROIs during 3 h. ROI 1 was not irradiated (control) and ROIs 2 and 3 were exposed to 5 mW for 10 min.

Due to the variations in the size of the cells at the start of the experiments, the NoP values were not directly comparable. Thus, the NoP for every data point was normalized by dividing with the area of the ROI at time $t=0$. This quantity was defined as the cell area index (CAI) and is simply given by

$$\text{CAI}(t) = \frac{\text{NoP}(t)}{\text{NoP}(t_0)},$$

which was directly comparable between ROIs. In all images, at least one control ROI was present, while the CAI was measured for all ROIs. Area growth for all control ROIs was exponential and showed good correlation between experiments (data not shown).

Using the CAI it was possible to calculate the maximum specific growth rate (μ_{max}) by fitting an exponential function, which also gave the doubling time $t_d = \ln 2 / \mu_{max}$ of the cell population within an ROI.

Using the area occupied by the cells for growth determination limited the time during which the cell growth could be followed accurately. We found that 3 to 4 h was the maximum time that the measured area of the ROIs could describe exponential growth. After this period, the cells would begin to bud vertically and the area did not increase exponentially. If ROIs began to form buds vertically with the time frame of the experiment, the ROIs were omitted from the analysis. For ROIs exposed to continuous irradiation, 15 to 20 ROIs were recorded for every power value with a total of 35 control

ROIs. For ROIs exposed to laser pulses, a minimum of 25 ROIs were recorded for every power value with a total of 40 control ROIs.

2.5 Calculation of Generation Time

To obtain growth kinetic data for the individual cells, we measured the generation time of the individual cells. The generation time was defined as the period between two consecutive buds from the same mother cell (Fig. 2). As images were taken at 2-min intervals, the temporal resolution of the time between two buds was ± 2 min. For all experiments, the generation times of both irradiated cells and control cells were obtained. For cells exposed to continuous irradiation, 20 to 30 cells were recorded for every power value with a total of 40 control cells. For cells exposed to laser pulses, 30 to 35 cells were recorded for every radiant flux value with a total number of 41 control cells.

2.6 Image Processing

All images were processed using LabVIEW 8.2 Vision software. A sharpening convolution kernel was applied first to enhance the contrast between the cell wall and background. Then local thresholding with background correction was applied. This left only the cell wall in the binary image. Due to the budding of daughter cells, the cell wall did not always form a complete circle after thresholding. Using the binary morphology (BM) operations “dilate” the cell walls were expanded with a number of iterations until they formed a complete circle. The BM operation “fill hole” was then used to fill the inside of the cell. To return the cells to normal size, the BM “erode” was then applied for same number of iterations as the BM operation “dilate.” Finally, to remove dust and cells touching the side, BM operations “remove small particles” and “remove border objects” were applied.

3 Results

3.1 Continuous Irradiation

The control cells exhibited exponential growth with a doubling time of 97 min (data not shown). As seen clearly in Fig. 3, all cells exposed to continuous laser light were inhibited in their growth and did not show exponential growth. After 1.5 h, the cells subjected to the lowest power (0.7 mW) were also significantly inhibited, but their growth rate increased slightly with time. The cells exposed to 1.3 mW were inhibited after 60 min and had a linear CAI increase, suggesting that the mother cells produced only a single daughter cell. The cells exposed to 2 mW were visibly inhibited after 60 min and the ROIs exposed to 2.6 mW were inhibited after 30 min. For both the 2- and 2.6-mW-exposed cells, the growth rate continuously declined and was close to zero after 3 h. However, the 2-mW-exposed cells leveled out at a higher CAI.

The variation of the generation times of individual mother cells increased with laser power (Fig. 4). However, absolute values for generation times were not attainable, as only cells that divided within the time frame of 5 h could be included in the measurement. The number of successful cell divisions within the 5-h period showed a continuous decline as a function of laser power with 100% cell division at 0.7 mW, 80%

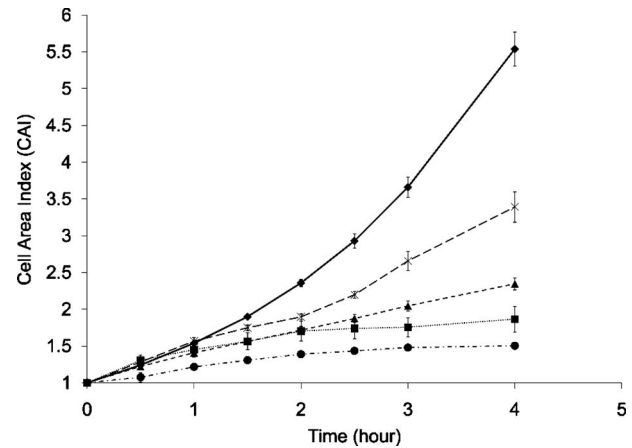


Fig. 3 Effect of continuous irradiation on CAI of *S. cerevisiae*: controls cells (◆), 0.7 mW (×), 1.3 mW (▲), 2.0 mW (■), and 2.6 mW (●). Data are means \pm standard error of the mean (SEM). Every data point in the control and irradiated ROI series is an average of between 35 and 15 to 20 measurements, respectively.

at 1.3 mW, 45% at 2.0 mW, and 0% cell division at 2.6 mW (data not shown). These results suggest that the measured generation times, and their variations, were increasingly underestimated with increasing laser power.

3.2 Pulsed Irradiation

To test whether the cell growth is affected only by the total dose received, we subjected cells to the same amount of energy but with different power; i.e., the cells subjected to 1, 5, and 10 mW were irradiated for 50, 10, and 5 min, respectively, after which cell growth was monitored. Thus, the total dose delivered to an average size cell was $D=3$ J. From Fig. 5 we observed that, although the total dose received was the same, the difference in the power through the cells clearly affected the CAI increase of the cells; i.e., the CAIs of 1-, 5-, and 10-mW exposures after 3 h were 89, 79, and 68%, respectively, of the control CAI.

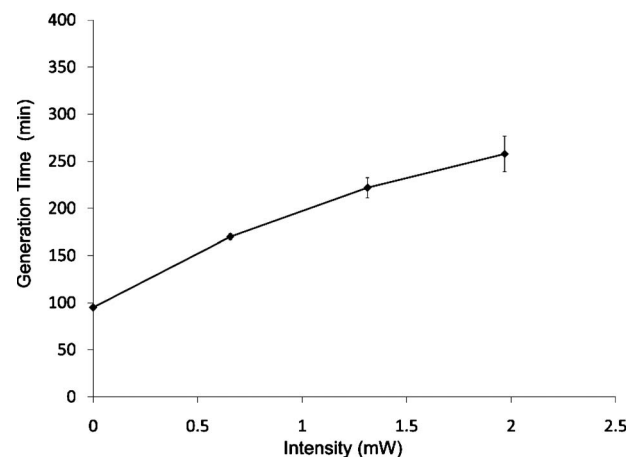


Fig. 4 Effect of continuous irradiation on percentage cell division of *S. cerevisiae* within the 5-h duration of the experiments. Control cells were not irradiated. Data points are means \pm SEM of 20 to 30 single cells.

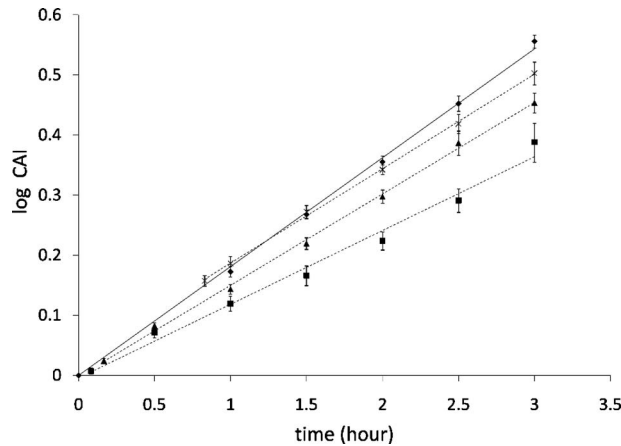


Fig. 5 Plot of log CAI as a function of time of pulsed irradiated *S. cerevisiae* cells. Control cells (\diamond) were not irradiated, 1 mW for 50 min (\times), 5 mW for 10 min (\blacktriangle), and 10 mW for 5 min (\blacksquare). The solid line is the exponential fit to the control data points starting a $t = 0$. The dashed lines are the exponential fits to the irradiated ROIs. The data points and the exponential fits for the 1-, 5-, and 10-mW exposures start after 50, 10, and 5 min, respectively, which indicate the end of the irradiation period. Data points are means \pm SEM of minimum 25 ROIs.

For all three pulses, the exposed cells recovered from the initial pulse and resumed exponential growth after the exposure period (Fig. 5, Table 1). To quantitatively examine how the cells recovered from the irradiation, exponential curves were fitted at the end of the irradiation period for the three different radiant flux series, and μ_{\max} and t_d were calculated from the CAI plots in Fig. 5. In the series with cells exposed to 1 mW for 50 min and 5 mW for 10 min, the exponential fits were good with $R^2 > 0.99$ and the two series had similar t_d values of 115 and 119 min, respectively, corresponding to approx. 120% of the control cells. Cells exposed to 10 mW for 5 min showed an even larger t_d value of 146 min, corresponding to 150% of the control cells; however, the fit was slightly worse than for cells exposed to 1 and 5 mW.

Note that because the cells were growing during exposure to the irradiation, the ROIs exposed to a low power for a long time received a larger dose than the ROIs exposed to a high power for a short time, simply due to the increase in area.

Using the data points in Fig. 5 to calculate the area under the curve by simple triangulation gives a total dose increase of 18% for ROIs exposed to 1 mW. For the cells exposed to 5 and 10 mW, the total dose increases are 1.7 and 0.7%, respectively. However, the consequence of correcting for the different total doses received by the cells would result in an even larger difference in growth between the exposed cells.

The generation times of pulse-irradiated individual mother cells within the ROIs were also recorded for the three different intensities (1, 5, and 10 mW) and the control cells (Table 1). The generation time of the cells was severely affected by the total dose, as it increased to 124 to 151% of the control cells. The cells exposed to 10 mW for 5 min had the largest increase (151%), while the cells exposed to 1 mW for 50 min were the least inhibited with a generation time increase of 124% as compared with the control.

As seen in Table 1, the generation time was significantly shorter than the t_d value of the control cells. However, this was not the case for the irradiated cells, where the generation time and the t_d were virtually similar.

4 Discussion

Our results clearly show that a power of 2.6 mW, which is 75% of the minimum effective trapping power of 3.5 mW for long-term continuous trapping in the BWS, will severely inhibit the growth of *S. cerevisiae* cells (Fig. 3). Furthermore, the number of successful divisions decreases rapidly with increasing laser power (data not shown). Most probably, longer exposure times than those applied in this study will even kill the cells. Even the lowest power of 0.7 mW inhibits the cell growth after 90 min (Fig. 3). This corresponds to a dose of 3.8 J to each individual cell. Furthermore, *S. cerevisiae* cells exposed to a power of 2.6 mW are clearly growth inhibited after only 30 min, corresponding to a received dose of 4.7 J. These results indicate that *S. cerevisiae* growth is dependent on the total dose received. Within the power regime studied here, there seems not to be a threshold power that triggers inhibition, but rather a continuous inhibition response to the accumulated dose (Figs. 3 and 4). These results correlate well with data from similar experiments done on other microorganisms,^{8,11} and they stress the fact that using lasers with a wavelength of 1070 nm to trap and manipulate *S. cer-*

Table 1 Growth data of pulsed irradiated *S. cerevisiae* cells.

Power Φ_{cell} (mW)	Exposure Time (min)	μ_{\max} (h^{-1}) ^a	R^2	Doubling Time (min.) ^b	Generation Time (min) ^c	Number of Cells (n) ^d
Control	0	0.4284	0.9989	97 (100)	92 \pm 2 (100)	45
1	50	0.3619	0.9991	115 (119)	114 \pm 4 (124)	35
5	10	0.3500	0.9984	119 (123)	121 \pm 6 (132)	34
10	5	0.3051	0.9864	146 (150)	139 \pm 9 (151)	30

^a μ_{\max} (h^{-1}) is the growth rate of the ROIs from the fit in Fig. 5, where R^2 is the correlation coefficient of the fit. The doubling time is calculated from μ_{\max} .

^bFor both the doubling time and the generation time, the relative change compared to the control is given in parenthesis.

^cThe generation time of mother cells are mean values \pm SEM.

^dThe number of mother cells (n) for each series used to measure the generation time.

evisiae cells over long time periods should be approached with great caution.

The results from Fig. 4 show an increased variation in generation time of irradiated cells with increasing laser power. This has also been observed for other microorganisms with other environmental stresses, such as heat and salt stress applied on single cells of *E. coli*.¹⁹ As one of the advantages of single-cell studies is the possibility to observe cell-to-cell variations not possible in bulk experiments, a decrease in laser power would not only result in less inhibition but also smaller cell-to-cell variations, thereby improving the quality of the quantitative data and minimizing acquisition times.

Whereas the *S. cerevisiae* cells exposed to continuous trapping are not able to grow exponentially, those that are exposed to the pulsed trapping conditions applied in this study resume exponential growth patterns after the trapping period (Fig. 5). However, all the exposed *S. cerevisiae* cells have lower μ_{\max} values with respect to the control cells (Table 1, Fig. 5). This indicates that growth of *S. cerevisiae* is permanently inhibited by the short-term exposures applied in this study.

Furthermore, our results clearly show that the growth of *S. cerevisiae* is not only dependent on the total dose received, as found here, but that it is also affected by the maximum power through the cell (Φ_{cell}) (Fig. 5, Table 1). This is consistent with Mohanty et al., who found DNA damage in human lymphoblasts to be dependent on both dose and maximum power.¹² However, our findings are in contrast to a recent study that found the viability of *E. coli* to be dependent only on the total dose received.¹⁰ This discrepancy is likely caused by the difference in the microorganism used, and the fact that Mirsaidov et al.¹⁰ studied cell viability, whereas we have focused on cell growth.

In this study, we measured the generation time of yeast mother cells. The generation time of a mother cell is generally shorter than of a daughter cell, as the daughter cell spends more time in the G1 unbudded phase,^{20,21} before the first bud is created. As t_d is a measure for the area increase of both the mother and the daughter cells, we would therefore expect that $t_d >$ the generation time. Comparing the t_d values with the generation times of the control cells in Table 1, we indeed find that the t_d is notably higher than the generation time. For the irradiated cells, however, we find comparable generation times and t_d values, indicating that the laser light somehow uncouples cell division from growth. These results are similar to recent studies that found¹¹ the generation time of *E. coli* cells to be more easily affected than the doubling time by laser light at 1064 nm. It is therefore possible that this phenomenon is a general microbial reaction to stress caused by photodamage.

The underlying mechanism for the photodamage has among others been proposed to be the formation of local heating.^{22,23} It is possible that the photodamage is caused by the local heating of specific organelles or components in the cell wall. However, we do not believe that the photodamage is caused by general heating of the cells, as the predicted temperature increase is minimal^{22,23} ($\Delta T < 1$ °C). Furthermore, a small increase in temperature would have had a favorable effect on the growth rate of *S. cerevisiae* cells, which was not observed.

As our results show, there seems to be a definite advantage to using the smallest possible power for trapping yeast cells by extending the trapping time (Fig. 5, Table 1). It is therefore pertinent to speculate whether a similar effect is present spatially, in which a trapped cell would be less inhibited by a homogeneous beam spread out over the whole cell rather than trapping with a highly focused beam. This hypothesis, however, should be further investigated.

In conclusion, we showed that the use of optical trapping at 1070 nm for direct control and manipulation of yeast cells has a significant impact on cell growth; i.e., it is not possible to continuously trap cells without severely inhibiting their growth. In contrast, yeast cells that are exposed to a defined dose are able to grow exponentially in a power-dependent manner; i.e., the lower the power, the higher the growth rate. Therefore, it may still be possible to conduct experiments with physiologically unaltered yeast cells on the BWS by using the minimum trapping power needed for trapping and restricting the exposure time to the absolute minimum.

Acknowledgments

This work was supported by the Danish Research Council for Technology and Production Sciences (FTP), Grant No. 274-05-0569.

References

1. E. R. Dufresne, G. C. Spalding, M. T. Dearing, S. A. Sheets, and D. G. Grier, "Computer-generated holographic optical tweezer arrays," *Rev. Sci. Instrum.* **72**(3), 1810–1816 (2001).
2. J. Glückstad, "Microfluidics—sorting particles with light," *Nature Mater.* **3**(1), 9–10 (2004).
3. P. J. Rodrigo, V. R. Daria, and J. Glückstad, "Four-dimensional optical manipulation of colloidal particles," *Appl. Phys. Lett.* **86**(7), 074103 (2005).
4. N. Arneborg, H. Siegumfeldt, G. H. Andersen, P. Nissen, V. R. Daria, P. J. Rodrigo, and J. Glückstad, "Interactive optical trapping shows that confinement is a determinant of growth in a mixed yeast culture," *FEMS Microbiol. Lett.* **245**(1), 155–159 (2005).
5. I. R. Perch-Nielsen, P. J. Rodrigo, and J. Glückstad, "Real-time interactive 3D manipulation of particles viewed in two orthogonal observation planes," *Opt. Express* **13**(8), 2852–2857 (2005).
6. A. Ashkin, J. M. Dziedzic, and T. Yamane, "Optical trapping and manipulation of single cells using infrared-laser beams," *Nature* **330**(6150), 769–771 (1987).
7. A. Dewith and K. O. Greulich, "Wavelength dependence of laser-induced DNA-damage in lymphocytes observed by single-cell gel-electrophoresis," *J. Photochem. Photobiol., B* **30**(1), 71–76 (1995).
8. H. Liang, K. T. Vu, P. Krishnan, T. C. Trang, D. Shin, S. Kimel, and M. W. Berns, "Wavelength dependence of cell cloning efficiency after optical trapping," *Biophys. J.* **70**(3), 1529–1533 (1996).
9. K. C. Neuman, E. H. Chadd, G. F. Liou, K. Bergman, and S. M. Block, "Characterization of photodamage to *Escherichia coli* in optical traps," *Biophys. J.* **77**(5), 2856–2863 (1999).
10. U. Mirsaidov, W. Timp, K. Timp, M. Mir, P. Matsudaira, and G. Timp, "Optimal optical trap for bacterial viability," *Phys. Rev. E* **78**(2), 021910 (2008).
11. S. Ayano, Y. Wakamoto, S. Yamashita, and K. Yasuda, "Quantitative measurement of damage caused by 1064-nm wavelength optical trapping of *Escherichia coli* cells using on-chip single cell cultivation system," *Biochem. Biophys. Res. Commun.* **350**(3), 678–684 (2006).
12. S. K. Mohanty, A. Rapp, S. Monajembashi, P. K. Gupta, and K. O. Greulich, "Comet assay measurements of DNA damage in cells by laser microbeams and trapping beams with wavelengths spanning a range of 308 nm to 1064 nm," *Radiat. Res.* **157**(4), 378–385 (2002).
13. M. B. Rasmussen, L. B. Oddershede, and H. Siegumfeldt, "Optical tweezers cause physiological damage to *Escherichia coli* and *Listeria bacteria*," *Appl. Environ. Microbiol.* **74**(8), 2441–2446 (2008).
14. K. Logg, K. Bodvard, A. Blomberg, and M. Kall, "Investigations on light-induced stress in fluorescence microscopy using nuclear local-

- ization of the transcription factor Msn2p as a reporter," *FEMS Yeast Res.* **9**(6), 875–884 (2009).
15. J. Glückstad, I. R. Perch-Nielsen, J. S. Dam, and D. Palima, "Biophotonics workstation," *Proc. SPIE* **6905**, 69050A (2008).
 16. J. S. Dam, I. R. Perch-Nielsen, D. Palima, and J. Glückstad, "Three-dimensional imaging in three-dimensional optical multi-beam micro-manipulation," *Opt. Express* **16**(10), 7244–7250 (2008).
 17. H.-U. Ulriksen, J. Thørgesen, S. Keiding, I. R. Perch-Nielsen, J. S. Dam, D. Palima, H. Stapelfeldt, and J. Glückstad, "Independent trapping, manipulation and characterization by an all-optical biophotonics workstation," *J. Eur. Opt. Soc. Rapid Publ.* **3**, 08034 (2008).
 18. H. Misawa, M. Koshioka, K. Sasaki, N. Kitamura, and H. Masuhara, "3-dimensional optical trapping and laser ablation of a single polymer latex particle in water," *J. Appl. Phys.* **70**(7), 3829–3836 (1991).
 19. G. W. Niven, J. S. Morton, T. Fuks, and B. A. Mackey, "Influence of environmental stress on distributions of times to first division in *Escherichia coli* populations, as determined by digital-image analysis of individual cells," *Appl. Environ. Microbiol.* **74**(12), 3757–3763 (2008).
 20. L. H. Hartwell and M. W. Unger, "Unequal division in *Saccharomyces cerevisiae* and its implications for control of cell-division," *J. Cell Biol.* **75**(2), 422–435 (1977).
 21. D. Porro, E. Martegani, B. M. Ranzi, and L. Alberghina, "Oscillations in continuous cultures of budding yeast—a segregated parameter analysis," *Biotechnol. Bioeng.* **32**(4), 411–417 (1988).
 22. Y. Liu, G. J. Sonek, M. W. Berns, and B. J. Tromberg, "Physiological monitoring of optically trapped cells: assessing the effects of confinement by 1064-nm laser tweezers using microfluorometry," *Biophys. J.* **71**(4), 2158–2167 (1996).
 23. E. J. G. Peterman, F. Gittes, and C. F. Schmidt, "Laser-induced heating in optical traps," *Biophys. J.* **84**(2), 1308–1316 (2003).